Model for the generation of toroidal and poloidal magnetic fields in a laser-produced plasma

B. Bhattacharyya,[1,2] Urmi Sanyal,[1] and S. V. Lawande[1,3]

[1]*Centre for Plasma Science and Technology, Department of Mathematics, University of North Bengal, Darjeeling 734 430, India*

[2]*TQE, Institut für Angewandte Physik, TH-Darmstadt, D-64289 Darmstadt, Germany*

[3]*Department of Physics, University of Pune, Pune 411007, India*

(Received 10 April 2000; published 21 December 2000)

A mechanism of simultaneous generation of toroidal and poloidal magnetic fields in an underdense region of a laser-produced plasma is discussed. The mechanism relies on the fact that at least a part of the incident transverse mode of the laser field undergoes a linear conversion into a longitudinal mode in the thermal plasma. It involves the conversion of ordered kinetic motion of the charged particles in the presence of the field into the energy of the induced magnetic fields both in poloidal and toroidal directions. The analysis is based on obtaining perturbative solutions of the two-fluid model of a hot nondissipative plasma. Our numerical results show that both the toroidal and poloidal fields increase with the laser intensity, and that the former dominates over the latter. Further, the toroidal fields decrease with increasing pulse lengths and increase rather slowly with an increase in laser wavelengths. However, the poloidal fields seem to be insensitive to the laser pulse lengths but they increase exponentially with the laser wavelengths. Finally, toroidal fields have a tendency to decrease as the critical surface is approached. The poloidal fields show a contrary behavior.

DOI: 10.1103/PhysRevE.63.016404 PACS number(s): 52.38.−r

I. INTRODUCTION

The generation of spontaneous magnetic fields in a laser-produced plasma is under continuous research because of their importance in pellet design in inertial confinement fusion (ICF). Various mechanisms have been proposed for the generation of large and small scale toroidal magnetic fields in laser produced plasmas [1–13]. Sources of large scale toroidal magnetic fields are the thermoelectric processes [1], the radiation processes [2,3], the rippled surface irregularities [4], the nonuniformities in laser intensity, and hot electron ejection from the focal spot [5,6] on one hand whereas, on the other hand, filamentation [7,8], resonance absorption [9–11], and the Weibel instability [12,13] are the sources of small scale toroidal magnetic fields. In fact, the sources of large or small scale poloidal magnetic fields are not properly understood yet. But, poloidal magnetic fields in the megagauss range are produced through the dynamo effect [14], ion-acoustic turbulence [15,16], and the induced magnetization arising out of the nonlinear optical response in plasmas [17–21]. Moreover, the gigagauss range poloidal magnetic field is produced through the ponderomotive force [22]. The various theoretical and experimental processes of the generation of toroidal and poloidal magnetic fields in laser-produced plasmas have been reviewed [23]. The effects of those fields on energy transport in ICF research have also been studied by many authors [24–29]. So far, from the available literature it appears that the generation of either toroidal or poloidal magnetic fields has been reported separately with supporting mechanisms. Recently [30], a model for the simultaneous generation of toroidal and poloidal magnetic fields by the interaction of an intense laser beam in an electron plasma has been discussed. In a realistic situation, the ion motion cannot be ignored. The present paper treats ion motion and its consequence effects. For a better understanding of the physics of magnetic-field generation in laser plasmas, various results are elucidated here graphically. It is shown that ion motion contributes substantially to the toroidal fields whereas the poloidal fields due to ions are nearly of the same order in magnitude and behave in the opposite direction to that of electrons.

The paper is organized as follows. In Sec. II the basic formulation of the problem is presented. In the same section the expressions for the nonlinear velocities of electrons and ions are derived, and also the components of nonlinear angular momentum (required for estimating the magnitude of toroidal and poloidal magnetic fields) are evaluated. In Sec. III the numerical results are explained graphically. Finally, in Sec. IV, some concluding remarks and a brief discussion are added to point out the importance of the simultaneous generation of poloidal and toroidal fields in implosion physics and also on spheromak. Some important derivations and the reason for exclusion of Landau damping effect are presented in Appendixes A and B, respectively.

II. FORMULATION OF THE PROBLEM

A. Basic assumptions and the relevant equations

The plasma is assumed to be a hot two-component fluid. Thermal velocities of electrons ($v_{\mathrm{th}e}$) and ions ($v_{\mathrm{th}i}$) are important in our analysis. For simplicity, the electron temperature T_e is taken to be equal to ion temperature T_i (i.e., $T_e = T_i = T$) and it is assumed that there is no temperature gradient ($\nabla T = 0$). Hence, the magnetic fields due to thermoelectric effect [1] are ignored. We treat the plasma as nondissipative by assuming that $(\nu/\omega) \ll 1$ where ν and ω are the collision and laser frequencies, respectively. Also assuming that the width of a resonance layer $\Delta x[\simeq(\nu/\omega)L$, where L is the density scale length] is small compared with the laser wavelength (λ_{ls}). So, the phenomena occuring at the resonance layer can be neglected [31]. Moreover, the inhomogeneity due to Landau damping has also been ignored because it is assumed that the electromagnetic wave number ($k_\perp$) is much greater than the electrostatic wave number ($k_\parallel$) [31].

Further assuming that the thermal velocities of electrons ($v_{\text{th}e}$) and ions ($v_{\text{th}i}$) are small compared with the phase velocity (v_φ) of the radiation field, and also that the Debye length (λ_D) is much less than the density scale length (L) of the plasma then the effect of plasma inhomogeneity may be neglected [32]. The very long density scale length ($L \gg \lambda_{ls} \gg \lambda_D$) and uniform temperature ($\nabla T = 0$) of the plasma indicate that the most beam energy are absorbed in the underdense plasma. The intensities of the incident waves are assumed to lie below the threshold value for the generation of inhomogeneities which gives rise to the self-action effects such as self-focussing, self-trapping, and self-phase modulation [33]. The intrinsic nonlinear instabilities due to SRS (stimulated Raman scattering) and SBS (stimulated Brillouin scattering) are also being neglected [32,33]. In the present formulation, we consider only Kerr-type nonlinearity [34,35] and hence a simple perturbation scheme [36] is used for all calculations.

To describe the interaction of laser fields with hot plasma, we consider the macroscopic behavior of the two-component plasma consisting of electrons and ions. So, the equations of continuity and momentum together with the usual Maxwell's equations can be written as

$$\dot{N}_e + \boldsymbol{\nabla} \cdot (N_e \dot{\mathbf{r}}_e) = 0, \tag{1}$$

$$\dot{N}_i + \boldsymbol{\nabla} \cdot (N_i \dot{\mathbf{r}}_i) = 0, \tag{2}$$

$$\ddot{\mathbf{r}}_e + (\dot{\mathbf{r}}_e \cdot \boldsymbol{\nabla}) \dot{\mathbf{r}}_e + \frac{e}{m_e}\mathbf{E} + \frac{e}{m_e c}(\dot{\mathbf{r}}_e \times \mathbf{H}) + \frac{\boldsymbol{\nabla} P_e}{m_e N_e} = \mathbf{0}, \tag{3}$$

$$\ddot{\mathbf{r}}_i + (\dot{\mathbf{r}}_i \cdot \boldsymbol{\nabla}) \dot{\mathbf{r}}_i - \frac{e}{m_i}\mathbf{E} - \frac{e}{m_i c}(\dot{\mathbf{r}}_i \times \mathbf{H}) + \frac{\nabla P_i}{m_i N_i} = \mathbf{0}, \tag{4}$$

$$\boldsymbol{\nabla} \times \mathbf{E} = -\left(\frac{\dot{\mathbf{H}}}{c}\right), \tag{5}$$

$$\boldsymbol{\nabla} \times \mathbf{H} = \left(\frac{\dot{\mathbf{E}}}{c}\right) + \frac{4\pi e}{c}(N_i \dot{\mathbf{r}}_i - N_e \dot{\mathbf{r}}_e), \tag{6}$$

$$\boldsymbol{\nabla} \cdot E = 4\pi e (N_i - N_e), \tag{7}$$

$$\boldsymbol{\nabla} \cdot \mathbf{H} = 0, \tag{8}$$

where $\mathbf{E}$, $\mathbf{H}$, N_e, N_i, $\dot{\mathbf{r}}_e$, $\dot{\mathbf{r}}_i$, m_e, and m_i are the electric field, the magnetic field, the electron density, the ion density, the electron velocity, the ion velocity, the electron mass, the ion mass, respectively and all other symbols have their usual meanings.

In order to complete the above set of equations, one needs to specify the equation of state for ions and electrons. For isothermal processes, the equations of state for electrons and ions are

$$P_e = N_e k_B T_e, \tag{9}$$

$$P_i = N_i k_B T_i, \tag{10}$$

where P_e, P_i, and k_B are the electron pressure, the ion pressure, and the Boltzmann constant, respectively.

The above set of equations (1)–(10) are to be solved by the successive approximation scheme [36]. In this scheme, any variable Φ is to be written as

$$\Phi = \Phi_0 + \varepsilon \Phi_1 + \varepsilon^2 \Phi_2 + \varepsilon^3 \Phi_3 + \cdots, \tag{11}$$

where Φ_0 represents the value in the unperturbed state or zero-order solution of Φ, Φ_1 the first order or the usual linear solution, while Φ_n is the nth-order approximation (for $n = 1,2,3,...$). In principle the parameter ε is a mathematical artifice [36,37] that allows us to compare the degree of approximation in a convenient way. In our case, however, $\boldsymbol{\epsilon}$ has a natural physical meaning of being the ratio of the electrons quiver speed (v_{osc}) to the speed of light (c). Nonlinearly excited third-order fields are to be solved in a closed form in which the first harmonic solutions are to be considered from their higher-order fields [37,38].

B. First-order fields and solutions

Let us assume that the linearized electric field in a hot plasma has the form [30]

$$\mathbf{E}_1 = (Mc\omega/2e)[\hat{\mathbf{x}}\alpha_\parallel e^{i\theta_\parallel} + (\hat{\mathbf{y}}\alpha_\perp - i\hat{\mathbf{z}}\beta_\perp)e^{i\theta_\perp}] + \text{c.c.}, \tag{12}$$

where $\alpha_\perp (= ea_\perp / Mc\omega)$, $\beta_\perp (= eb_\perp / Mc\omega)$ are the dimensionless amplitudes of the transverse electric field $\alpha_\parallel$ ($= a_\parallel e/Mc\omega$) is that of longitudinal field, $\theta_\perp = k_\perp x - \omega t$ and $\theta_\parallel = k_\parallel x - \omega t$ are two phases, $k_\perp$ and $k_\parallel$ are the transverse and the longitudinal wave numbers, respectively, ω is the frequency of the wave, $M[= m_e m_i/(m_e + m_i)]$ is the mean mass, $\hat{\mathbf{x}}$, $\hat{\mathbf{y}}$, and $\hat{\mathbf{z}}$ are the unit vectors along the three mutually perpendicular directions and c.c. represents the complex conjugate. In Eq. (12), the last two terms in the third bracket arise directly from the laser fields while the first component arises from the converted mode [31]. The justifications for using the form of the linearized electric field of Eq. (12) are explained in Sec. IV and also in Appendix B.

Using Eq. (12) in the set of linearized equations (1)–(10), we have the linearized velocities of electrons and ions as

$$\dot{\mathbf{r}}_{e1} = i(M_e c/2)[D_{e1}\hat{\mathbf{x}}\alpha_\parallel e^{i\theta_\parallel} + D_{e2}(\hat{\mathbf{y}}\alpha_\perp - i\hat{\mathbf{z}}\beta_\perp)e^{i\theta_\perp}] + \text{c.c.} \tag{13}$$

and

$$\dot{\mathbf{r}}_{i1} = i(M_i c/2)[D_{i1}\hat{\mathbf{x}}\alpha_\parallel e^{i\theta_\parallel} + D_{i2}(\hat{\mathbf{y}}\alpha_\perp - i\hat{\mathbf{z}}\beta_\perp)e^{i\theta_\perp}] + \text{c.c.}, \tag{14}$$

where

$$D_{e1} = 1 - V_i^2 G_e n_\parallel / 2M_i, \quad D_{e2} = (n_\perp^2 - 1)/X, \quad M_e = M/m_e,$$

and

$$D_{i1} = 1 - V_e^2 G_i n_\parallel / 2M_e, \quad D_{i2} = D_{e2}, \quad M_i = M/m_i.$$

The linearized densities of electrons and ions are

$$N_{e1}=i(N_0/2)[G_e\alpha_\parallel e^{i\theta_\parallel}-\text{c.c.}], \tag{15}$$

$$N_{i1}=i(N_0/2)[G_i\alpha_\parallel e^{i\theta_\parallel}-\text{c.c.}], \tag{16}$$

where

$$G_e=[2(X-1)+V_e^2n_\parallel^2]/[n_\parallel(V_i^2-V_e^2)],$$

and

$$G_i=[2(X-1)+V_i^2n_\parallel^2]/[n_\parallel(V_i^2-V_e^2)].$$

Also the linearized magnetic field is

$$\mathbf{H}_1=(Mc\omega/2e)[(i\hat{\mathbf{y}}\beta_\perp+\hat{\mathbf{z}}\alpha_\perp)n_\perp e^{i\theta_\perp}]+\text{c.c.} \tag{17}$$

C. Preliminary analysis

Using Eq. (12) in the linearized equations (1)–(10), we have the linearized dispersion relation for transverse waves as

$$n_\perp^2-1\times X_p=0, \tag{18}$$

where

$$n_\perp=k_\perp c/\omega,\quad X_p=X_i+X_e,\quad X_e=\omega_{pe}^2/\omega^2,\quad X_i=\omega_{pi}^2/\omega^2,$$

$$\omega_{pe}^2=4\pi N_0e^2/m_e,\quad \omega_{pi}^2=4\pi N_0e^2/m_i,$$

and that for longitudinal waves as

$$[(V_i^2n_\parallel^2/2)-1][(V_e^2n_\parallel^2/2)-1]+X_i[(V_e^2n_\parallel^2/2)-1]$$
$$+X_e[(V_i^2n_\parallel^2/2)-1]=0, \tag{19}$$

where $n_\parallel=k_\parallel c/\omega$, $V_e^2=v_{\text{the}}^2/c^2$, $V_i^2=v_{\text{th}i}^2/c^2$, $v_{\text{the}}^2=2kT_0/m_e$, $v_{\text{th}i}^2=2T_0/m_i$.

The above two linear dispersion relations (18) and (19) are not coupled. So, the exchange of energy between transverse and longitudinal waves at the time of their propagation in the plasma is not possible in the linear case. It is also clear that the dispersion relations for both the waves are independent of their wave amplitudes. Moreover, the linearized dispersion relation (18) for the transverse component is free from thermal velocities of charged particles whereas the longitudinal dispersion relation (19) depends on thermal velocities of those particles.

D. Second-order fields and solutions

Using Eqs. (12)–(16) in the second-order field equations (1)–(10), the nonlinear excited second-order electric field $\mathbf{E}_2$ is obtained as

$$\mathbf{E}_2=i(Mc\omega/2e)\{\hat{\mathbf{x}}[\xi_\parallel\alpha_\parallel^2e^{2i\theta_\parallel}+\xi_\perp(\alpha_\perp^2-\beta_\perp^2)e^{2i\theta_\parallel}]$$
$$+\xi(\hat{\mathbf{y}}\alpha_\perp-i\hat{\mathbf{z}}\beta_\perp)\alpha_\parallel e^{i(\theta_\perp+\theta_\parallel)}\}+\text{c.c.}, \tag{20}$$

where

$$\xi_\parallel=-2(P_{1\parallel}/Q_{1\parallel}),\quad \xi_\perp=-2(P_{1\perp}/Q_{1\perp}),\quad \xi=2(P_1/Q_1)$$

and also

$$P_{1\parallel}=XG_1[(V_i^2n_\parallel^2/2)-1][(V_e^2n_\parallel^2/2)-1]$$
$$+(X/4)[(V_e^2n_\parallel^2/2)-1]\tau_{i\parallel}+(X/4)[(V_i^2n_\parallel^2/2)-1]\tau_{e\parallel},$$

$$Q_{1\parallel}=4[(V_i^2n_\parallel^2/2)-1][(V_e^2n_\parallel^2/2)-1]+X_i[(V_e^2n_\parallel^2/2)-1]$$
$$+X_e[(V_i^2n_\parallel^2/2)-1],$$

$$P_{1\perp}=-(X/4)[(V_e^2n_\perp^2)-1]\tau_{i\perp}+(X/4)[(V_i^2n_\perp^2/2)-1]\tau_{e\perp},$$

$$Q_{1\perp}=4[(V_i^2n_\perp^2/2)-1][(V_e^2n_\perp^2/2)-1]+X_i[(V_e^2n_\perp^2/2)-1]$$
$$+X_e[(V_i^2n_\perp^2/2)-1],$$

$$P_1=XG,\quad Q_1=(n_\parallel+n_\perp)^2-4+X_e+X_i,$$

$$G_1=\tfrac{1}{2}(M_iG_eD_e+M_eG_iD_i),\quad G=\tfrac{1}{2}(M_iG_e+M_eG_i),$$

$$\tau_{e\parallel}=\sigma_en_\parallel+G_iD_iV_e^2M_en_\parallel^2,\quad \tau_{e\perp}=M_e^2n_\perp,$$

$$\tau_{i\parallel}=\sigma_in_\parallel+G_eD_eV_i^2M_in_\parallel^2,\quad \tau_{i\perp}=M_i^2n_\perp,$$

$$\sigma_e=M_e^2D_i^2-V_e^2G_i^2/2,\quad \sigma_i=M_i^2D_e^2-V_i^2G_e^2/2.$$

The expression of the second-order magnetic field $\mathbf{H}_2$ is

$$\mathbf{H}_2=-(Mc\omega/2e)[(\hat{\mathbf{y}}\beta_\perp-i\hat{\mathbf{z}}\alpha_\perp)\xi\alpha_\parallel e^{i(\theta_\perp+\theta_\parallel)}]+\text{c.c.} \tag{21}$$

Also the velocities of electrons ($\dot{\mathbf{r}}_{e2}$) and of ions ($\dot{\mathbf{r}}_{i2}$) are the forms

$$\dot{\mathbf{r}}_{e2}=(c/2)\{\hat{\mathbf{x}}[\eta_\parallel\alpha_\parallel^2e^{2i\theta_\parallel}+\eta_\perp(\alpha_\perp^2-\beta_\perp^2)e^{2i\theta_\perp}]$$
$$+\eta(\hat{\mathbf{y}}\alpha_\perp-i\hat{\mathbf{z}}\beta_\perp)\alpha_\parallel e^{i(\theta_\perp+\theta_1)}\}+\text{c.c.}, \tag{22}$$

$$\dot{\mathbf{r}}_{i2}=(c/2)\{\hat{\mathbf{x}}[\zeta_\parallel\alpha_\parallel^2e^{2i\theta_\parallel}+\zeta_\perp(\alpha_\perp^2-\beta_\perp^2)e^{2i\theta_\perp}]$$
$$+\zeta(\hat{\mathbf{y}}\alpha_\perp-i\hat{\mathbf{z}}\beta_\perp)\alpha_\parallel e^{i(\theta_\perp+\theta_\parallel)}\}+\text{c.c.}, \tag{23}$$

where

$$\eta_\parallel=\tfrac{1}{4}(P_{e\parallel}/Q_{1\parallel}),\quad \eta_\perp=\tfrac{1}{4}(P_{e\perp}/Q_{1\perp}),\quad \eta=\tfrac{1}{4}(P_e/Q_1),$$

and

$$\zeta_\parallel=\tfrac{1}{4}(P_{i\parallel}/Q_{1\parallel}),\quad \zeta_\perp=\tfrac{1}{4}(P_{i\perp}/Q_{1\perp}),\quad \zeta=\tfrac{1}{4}(P_i/Q_1),$$

and also

$$P_e=-4X_eG,\quad P_i=-4X_iG,$$

$$P_{e\parallel}=-\{4[(V_i^2n_\perp^2/2)-1]+X_i\}\tau_{e\parallel}$$
$$+X_e\tau_{i\parallel}+4X_e[(V_i^2n_\parallel^2/2)-1]G_1,$$

$$P_{e\perp}=-\{4[(V_i^2n_\perp^2/2)-1]+X_i\}\tau_{e\perp}+X_e\tau_{i\perp},$$

$$P_{i\parallel}=-\{4[(V_e^2n_\perp^2/2)-1]+X_e\}\tau_{i\parallel}$$
$$+X_i\tau_{e\parallel}+4X_i[(V_e^2n_\parallel^2/2)-1]G_1,$$

$$P_{i\perp}=-\{4[(V_e^2n_\perp^2/2)-1]+X_e\}\tau_{i\perp}+X_i\tau_{e\perp}\,,$$

The excited electron and ion densities are

$$N_{e2}=(N_0/2)[S_{e\parallel}\alpha_\parallel^2e^{2i\theta_\parallel}+S_{e\perp}(\alpha_\perp^2-\beta_\perp^2)e^{2i\theta_\perp}]+\text{c.c.}, \tag{24}$$

$$N_{i2}=(N_0/2)[S_{i\parallel}\alpha_\parallel^2e^{2i\theta_\parallel}+S_{i\perp}(\alpha_\perp^2-\beta_\perp^2)e^{2i\theta_\perp}]+\text{c.c.}, \tag{25}$$

where

$$S_{e\parallel}=(\eta_\parallel-M_eG_iD_i/2)n_\parallel\,,\quad S_{e\perp}=\eta_\perp n_\perp\,,$$

and

$$S_{i\parallel}=(-\zeta_\parallel+M_iG_eD_e/2)n_\parallel\,,\quad S_{i\perp}=-\zeta_\perp n_\perp\,.$$

It is evident that the linearized solutions (given in Sec. II B) contain first-order harmonic terms. But the second-order solutions (derived in this section) contribute only second-order harmonic terms. Hence, in the absence of the first-order harmonic terms the nonlinearly excited second-order fields do not contribute a dc magnetic field. Moreover, in our calculations, plasma inhomogeneity, field fluctuation, and collisional effects have been ignored. Thus, the second-order solenoidal wave field does not generate a magnetic field. Hence, the nonlinearly excited third-order field variables are to be explored for possible magnetic-field generation by our mechanism.

E. Equations for third-order fields and their solutions

From Eqs. (1)–(10), we deduce the following three basic partial-differential equations of third order:

$$(c^2\nabla^2-c^2\,\text{grad div}-D_t^2)\mathbf{E}_3-4\pi eN_0D_t^2\mathbf{r}_{i3}+4\pi eN_0D_t^2\mathbf{r}_{e3}=\mathbf{T}_{\rm NEE}, \tag{26}$$

$$(e/m_e)D_t\mathbf{E}_3+D_t[D_t^2-(v_{\rm the}^2/2)\text{grad div}]\mathbf{r}_{e3}=\mathbf{T}_{\rm NLE}, \tag{27}$$

and

$$-(e/m_i)D_t\mathbf{E}_3+D_t[D_t^2-(\nu_{\rm thi}^2/2)\text{grad div}]\mathbf{r}_{i3}=\mathbf{T}_{\rm NLI}, \tag{28}$$

where $\mathbf{T}_{\rm NEE}$, $\mathbf{T}_{\rm NLE}$, and $\mathbf{T}_{\rm NLI}$ are the nonlinear third-order terms. They have the following forms:

$$\mathbf{T}_{\rm NEE}=4\pi eD_t[(N_{i1}\dot{\mathbf{r}}_{i2}-N_{e1}\dot{\mathbf{r}}_{e2})+(N_{i2}\dot{\mathbf{r}}_{i1}-N_{e2}\dot{\mathbf{r}}_{e1})],$$

$$\begin{aligned}\mathbf{T}_{\rm NLE}=&-D_t[(\dot{\mathbf{r}}_{e1}\cdot\nabla)\dot{\mathbf{r}}_{e2}+(\dot{\mathbf{r}}_{e2}\cdot\nabla)\dot{\mathbf{r}}_{e1}\\&+(e/M_ec)(\dot{\boldsymbol{\gamma}}_{e1}\times\mathbf{H}_2)+(e/M_ec)(\dot{\mathbf{r}}_{e2}\times\mathbf{H}_1)]\\&+[(v_{\rm the}^2/2N_0)\text{grad div}(N_{e1}\dot{\mathbf{r}}_{e2}+N_{e2}\dot{\mathbf{r}}_{e1})]\\&+D_t(v_{\rm the}^2/2N_0^2)[-(N_{e1}^2/N_0)\text{grad div}\,N_{e1}\\&+N_{e2}\,\text{grad div}\,N_{e1}+N_{e1}\,\text{grad div}\,N_{e2}],\end{aligned}$$

$$\begin{aligned}\mathbf{T}_{\rm NLI}=&-D_t[(\dot{\mathbf{r}}_{i1}\cdot\nabla)\dot{\mathbf{r}}_{i2}+(\dot{\mathbf{r}}_{i2}\cdot\nabla)\dot{\mathbf{r}}_{i1}-(e/M_ic)(\dot{\mathbf{r}}_{i1}\times\mathbf{H}_2)\\&-(e/M_ic)(\dot{\mathbf{r}}_{i2}\times\mathbf{H}_1)]+[(v_{\rm thi}^2/2N_0)\text{grad div}(N_{i1}\dot{\mathbf{r}}_{i2}\\&+N_{i2}\dot{\mathbf{r}}_{i1})]+D_t(v_{\rm thi}^2/2N_0^2)[-(N_{i1}^2/N_0)\text{grad div}\,N_{i1}\\&+N_{i2}\,\text{grad div}\,N_{i1}+N_{i1}\,\text{grad div}\,N_{i2}].\end{aligned}$$

The terms in the square bracket of $\mathbf{T}_{\rm NEE}$ are due to plasma current for the electron and ion. The first two terms in the first square bracket of $\mathbf{T}_{\rm NLE}$ comes from the substantial derivative of the electron momentum; the last two terms in the same bracket represent the Lorentz force for electron. The terms in the second square bracket of $\mathbf{T}_{\rm NLE}$ are due to the substantial derivative of the electron continuity equation. All other terms in the last square bracket of $\mathbf{T}_{\rm NLE}$ are due to the pressure gradient of electrons. In a similar way, all the nonlinear terms of $\mathbf{T}_{\rm NLI}$ contained in the square brackets can be explained due to ion motion in a plasma continuum.

Solving Eqs. (26), (27), and (28) by Cramer's rule and retaining only first-order harmonic terms, we have the following expressions for the nonlinear velocity of the electron ($\dot{\mathbf{r}}_{e3}$):

$$\begin{aligned}\dot{\mathbf{r}}_{e3}=&\,i(c/2)\{\hat{\mathbf{x}}[R_{11}\alpha_\parallel^3e^{i\theta_\parallel}+R_{12}(\alpha_\perp^2-\beta_\perp^2)\alpha_\parallel e^{i(2\theta_\perp-\theta_\parallel)}\\&+R_{13}(\alpha_\perp^2+\beta_\perp^2)\alpha_\parallel e^{i\theta_\parallel}]+\hat{\mathbf{y}}[R_{21}\alpha_\parallel^2\alpha_\perp e^{i(2\theta_\parallel-\theta_\perp)}\\&+R_{22}(\alpha_\perp^2-\beta_\perp^2)\alpha_\perp e^{i\theta_\perp}+R_{23}\alpha_\parallel^2\alpha_\perp e^{i\theta_\perp}]\\&-i\hat{\mathbf{z}}[R_{31}\alpha_\parallel^2\beta_\perp e^{i(2\theta_\parallel-\theta_\perp)}+R_{32}(\alpha_\perp^2-\beta_\perp^2)\beta_\perp e^{i\theta_\perp}\\&+R_{33}\alpha_\parallel^2\beta_\perp e^{i\theta_\perp}]\}+\text{c.c.}\end{aligned} \tag{29}$$

and that of the ion ($\dot{\mathbf{r}}_{i3}$)

$$\begin{aligned}\dot{\mathbf{r}}_{i3}=&\,i(c/2)\{\hat{\mathbf{x}}[T_{11}\alpha_\parallel^3e^{i\theta_\parallel}+T_{12}(\alpha_\perp^2-\beta_\perp^2)\alpha_\parallel e^{i(2\theta_\perp-\theta_\parallel)}\\&+T_{13}(\alpha_\perp^2+\beta_\perp^2)\alpha_\parallel e^{i\theta_\parallel}]+\hat{\mathbf{y}}[T_{21}\alpha_\parallel^2\alpha_\perp e^{i(2\theta_\parallel-\theta_\perp)}\\&+T_{22}(\alpha_\perp^2-\beta_\perp^2)\alpha_\perp e^{i\theta_\perp}+T_{23}\alpha_\parallel^2\alpha_\perp e^{i\theta_\perp}]\\&-i\hat{\mathbf{z}}[T_{31}\alpha_\parallel^2\beta_\perp e^{i(2\theta_\parallel-\theta_\perp)}+T_{32}(\alpha_\perp^2-\beta_\perp^2)\beta_\perp e^{i\theta_\perp}\\&+T_{33}\alpha_\parallel^2\beta_\perp e^{i\theta_\perp}]\}+\text{c.c.},\end{aligned} \tag{30}$$

where values of all R's and T's are written in Appendix A. Henceforth, the subscript 3 will be dropped from all the third-order nonlinear terms. It is a fact that the nondissipative plasma approximation demands the real values of wave number (k) and frequency (ω) of the radiation fields which entrusts to avoid field fluctuations and collisional effects in our calculations.

F. Nonlinear angular momentum and magnetization

The total nonlinear magnetic moments for electrons and ions turn out as

$$\boldsymbol{\mu}=\boldsymbol{\mu}_e+\boldsymbol{\mu}_i\,, \tag{31}$$

where $\boldsymbol{\mu}_e$ and $\boldsymbol{\mu}_i$ are the nonlinear electronic and ionic magnetic moments, respectively, and can be expressed as

$$\boldsymbol{\mu}_e=(\mathbf{r}_e\times\mathbf{j}_e)/2c \quad \text{and} \quad \boldsymbol{\mu}_i=(\mathbf{r}_i\times\mathbf{j}_i)/2c, \tag{32}$$

where $\mathbf{j}_e$ and $\mathbf{j}_i$ are the nonlinear current vectors due to electrons and ions, respectively. The expressions of $\mathbf{j}_e$ and $\mathbf{j}_i$ are given by

$$\mathbf{j}_e=-e\dot{\mathbf{r}}_e \quad \text{and} \quad \mathbf{j}_i=e\dot{\mathbf{r}}_i. \tag{33}$$

The nonlinear electron and ion velocities $\dot{\mathbf{r}}_e$ and $\dot{\mathbf{r}}_i$ are given in Eqs. (29) and (30), respectively, and their displacements $\mathbf{r}_e$ and $\mathbf{r}_i$ are defined in Eqs. (A1) and (A2). The nonlinear angular momentum for two-component plasmas is given by

$$\mathbf{L}=(2c/e)(\boldsymbol{\mu}_i-\boldsymbol{\mu}_e). \tag{34}$$

So, the nonlinear induced magnetization in laser plasmas, averaged over the fast laser frequency time scale (i.e., $2\pi/\omega$) can be expressed as

$$\langle M\rangle=(4\pi eN_0/c)(\langle\mu_i\rangle-\langle\mu_e\rangle)=\langle M_i\rangle+\langle M_e\rangle, \tag{35}$$

where $\langle M_e\rangle$ and $\langle M_i\rangle$ are the averaged induced magnetization for electrons and ions, respectively.

The total averaged induced poloidal magnetic fields for electrons and ions in the x direction (i.e., the direction of the wave propagation or, in other words, the direction of the laser beam) can be expressed as

$$M_p=(\langle M_{ex}\rangle+\langle M_{ix}\rangle). \tag{36}$$

The resultant of both y and z components of induced magnetization for electrons and ions turns out to be the total toroidal magnetic fields. It will be in a plane perpendicular to the direction of laser beams. The resultant toroidal magnetic field can be expressed as

$$M_t=[(\langle M_{iy}\rangle)^2+(\langle M_{iz}\rangle)^2+(\langle M_{ey}\rangle)^2+(\langle M_{ez}\rangle)^2]. \tag{37}$$

III. GRAPHICAL ILLUSTRATION ON NUMERICAL RESULTS

The numerical estimations of both the toroidal and poloidal magnetic fields have been made for the Nd-glass laser with wavelengths in μm, pulse lengths in ns, and intensities in W/cm^2. The thermal power flux is $5(1+1/Z)(Nk_BT)\times(\Delta R/\tau)$ W/cm^2, where Z, k_BT, τ, N, and R are the effective ionic charge number, the plasma temperature in eV, the laser pulse lengths in ns, the density in cm^{-3}, and the spot radius R in μm, respectively. The region of our interest has been assumed to be composed of slabs, and the length ΔR of each slab is so chosen such that the temperature in that slab is fairly constant and the mean value of the density can reasonably be taken. The induced magnetic fields have been calculated on the basis of those values of temperature and density. Numerical results show that the induced toroidal magnetic field is not maximum at the critical density but well below it as in Fig. 1(a). These results are consistent with the experimental results [5] and numerically computed results [39]. But, Fig. 1(b) tells us that the position of the peak value of the poloidal fields is near the critical density, which is yet to be verified either by experiment or by simulation. The magnitudes of toroidal and poloidal fields are different in different plasma expansion regions. So, their Larmor radius effects on the rate of energy deposition in conduction regions would be different and hence, the effect of energy transport from a critical surface to an ablation surface is not uniform. More studies are needed of energy transport for such fields. Figure 2(a) shows that the toroidal field decreases with increasing pulse length but the poloidal field has no change as shown in Fig. 2(b). Figures 3(a) and 3(b) show that magnetic fields will increase with increasing laser intensities. These results agree with earlier results [1,2,4,5,11,14,16,17,19]. Figure 4(a) points out that toroidal fields increase very slowly with an increase in the wavelength, but poloidal fields increase exponentially as shown in Fig. 4(b). A rough sketch in Fig. 5 shows the region of the underdense plasma where our model for the generation of magnetic fields may be valid.

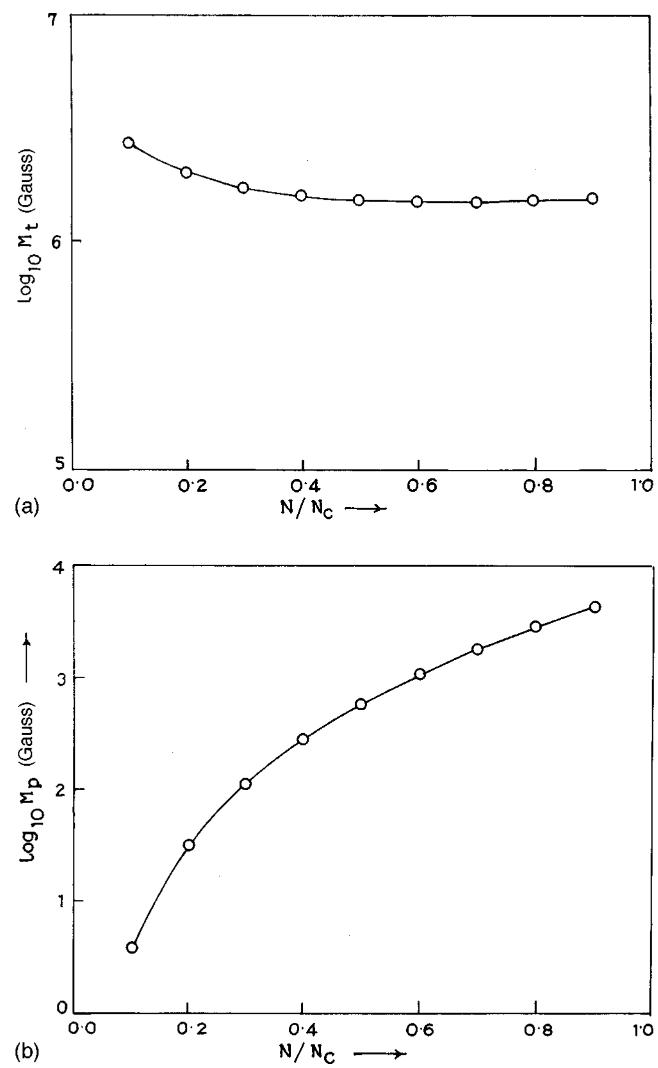

FIG. 1. (a) Variation of the logarithmic values of the toroidal magnetic fields in gauss ($\log_{10} M_t$) with the density ratio (N/N_c) at $\tau=5$ ns, $\lambda=1.06$ μm, $I=10^{15}$ W/cm^2. (b) Variation of the logarithmic values of the poloidal magnetic fields in gauss ($\log_{10} M_p$) with the density ratio (N/N_c) at $\tau=5$ ns, $\lambda=1.06$ μm, $I=10^{15}$ W/cm^2.

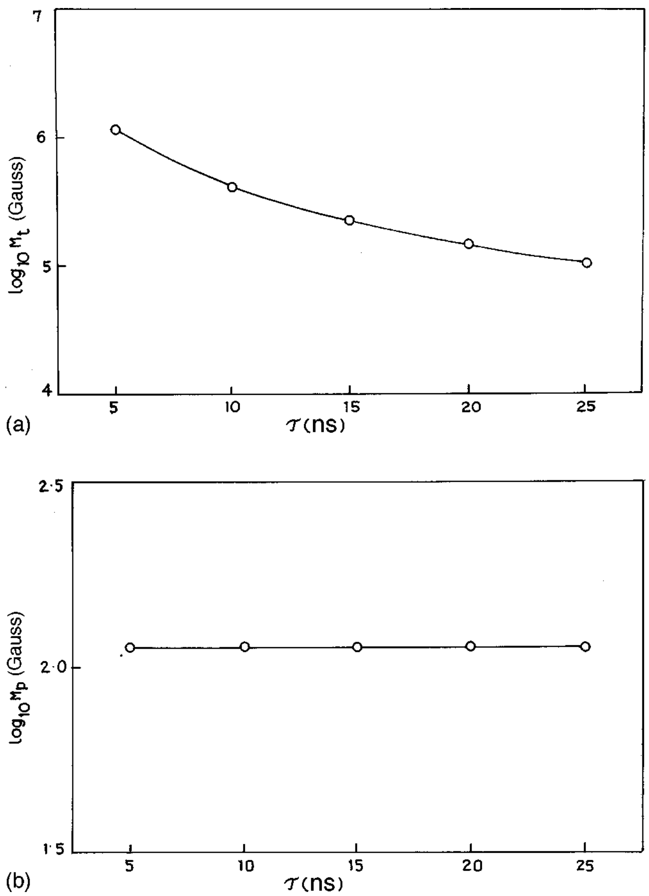

FIG. 2. (a) The variation of the logarithmic values of the toroidal magnetic fields in gauss ($\log_{10} M_t$) with the pulse length (τ) in ns at $(N/N_c)=0.3$, $\lambda=1.06\ \mu$m, $I=10^{15}$ W/cm^2. (b) Variation of the logarithmic values of the poloidal magnetic fields in gauss ($\log_{10} M_p$) with the pulse length (τ) in ns at $(N/N_c)=0.3$, $\lambda=1.06\ \mu$m, $I=10^{15}$ W/cm^2.

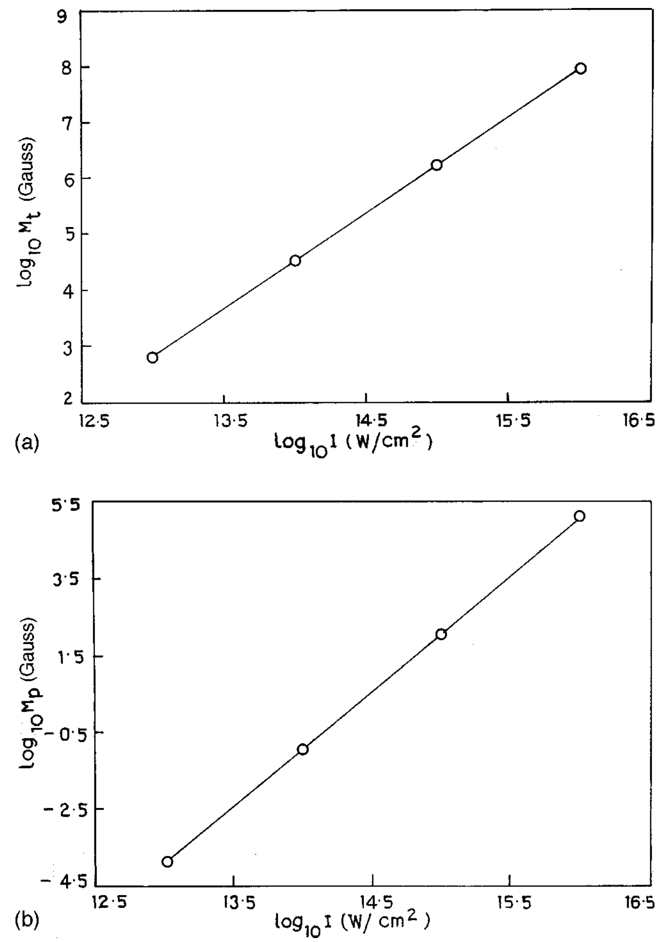

FIG. 3. (a) Variation of the logarithmic values of the toroidal magnetic fields in gauss ($\log_{10} M_t$) with the logarithmic laser intensity (I) in W/cm^2 at $\tau=5$ ns, $(N/N_c)=0.3$, $\lambda=1.06\ \mu$m. (b) Variation of the logarithmic values of the poloidal magnetic fields in gauss ($\log_{10} M_p$) with the logarithmic laser intensity (I) in W/cm^2 at $\tau=5$ ns, $(N/N_c)=0.3$, $\lambda=1.06\ \mu$m.

It is better to point out here that out of 80-μm density scale length the thickness of the resonance layer is of the order of 1 μm and the length of influence of Landau damping is approximately 24 μm. Hence, the typical length of the region of interest for field generation is about 55 μm only. In fact, one can modify our results by incorporating the effects of resonance layer and Landau damping.

IV. CONCLUDING REMARKS

We have proposed here a mechanism of the simultaneous generation of poloidal and toroidal magnetic fields in a one-temperature (i.e., $T_e=T_i=T$), two-component, and nondissipative plasma. This mechanism originates from the transformation of kinetic energies of the ordered motion of charged particles, in the presence of the wave, into the energy of the induced magnetic fields both in poloidal and in toroidal directions. Such toroidal and poloidal fields are dc over the fast laser time scale (i.e., $2\pi/\omega$). But for measuring such fields in a laboratory, the field should be dc for longer time scales, viz., laser pulse length (5 ns, say) or the hydrodynamic time scale ($=L/\nu_{\mathrm{th}i}$, where L is the characteristic length and $\nu_{\mathrm{th}i}$ is the ion acoustic velocity). Even for such a longer time scale our results do not show any qualitative change because of the fact that the effects of ion motion and moderate laser intensity have been taken into account for our field generation studies.

The electromagnetic mode of a p-polarized laser light can be converted to the electrostatic mode at the critical density N_c, when its electric vector oscillates along the direction of the density gradient. This effect is known as resonance absorption [32] which also gives rise to the magnetic field in plasmas [9–11]. We exclude such an effect in our calculations because our interest is in calculating the magnetic fields in underdense regions.

Kull [31] has shown that the mode conversion is possible even in the underdense region if the thermal plasma is present, and has also pointed out that the width of the conversion layer (here we call it a resonance layer) plays an important role in such conversion. Thus, the amplitude of the electromagnetic mode of the laser light will be modified by thermal plasma and, so, the linearized form of the electric fields in Eq. (12) is justified for the region of our interest.

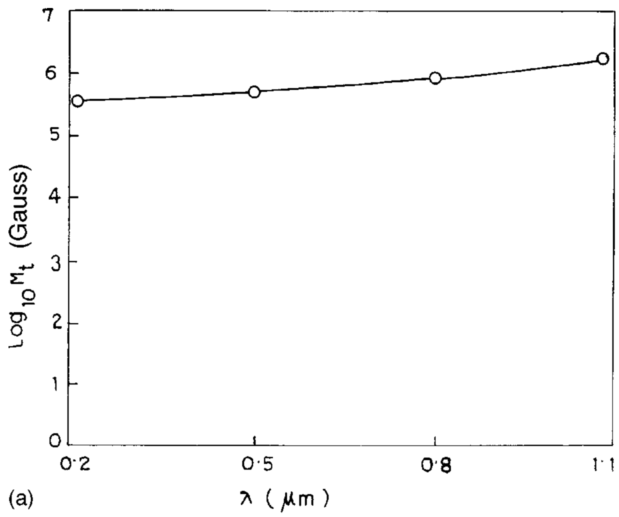

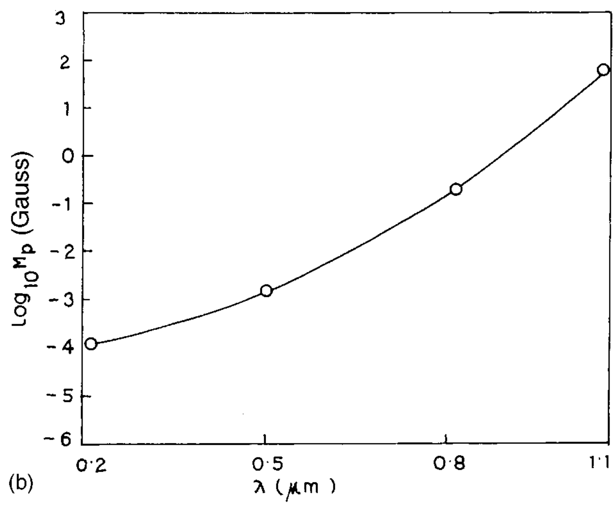

FIG. 4. (a) Variation of the logarithmic values of the toroidal magnetic fields in gauss ($\log_{10} M_t$) with the laser wavelength (λ) in μm at $(N/N_c)=0.3$, $\tau=5$ ns, $I=10^{15}$ W/cm^2. (b) Variation of the logarithmic values of the poloidal magnetic fields in gauss ($\log_{10} M_p$) with the laser wavelength (λ) in μm at $(N/N_c)=0.3$, $\tau=5$ ns, $I=10^{15}$ W/cm^2.

Further, it may also be noted that this model should have the following three limitations.

(a) Let $(\nu/\omega)(L/\lambda_{ls})\simeq 0.01$ which gives $\Delta x/\lambda_{ls}\ll 1$, where the width of the resonance layer is $\Delta x[=(\nu/\omega)L]$, where ν is the collision frequency and L is the density scale length. Hence, the phenomena which occur at the resonance layer have been ignored.

(b) The inhomogeneity due to Landau damping has also been ignored. Since $k_{\parallel}\lambda_D<1$, and $k_{\perp}/k_{\parallel}\ll 1$, where $k_{\parallel}$ $(=k_0\sqrt{\epsilon}/\beta)$ is the electrostatic wave number, $k_{\perp}(=k_0\sqrt{\epsilon})$ is the electromagnetic wave number, and $k_0(=\omega/c)$ is the vacuum wave number, $\beta[=(\nu_{\text{the}}+\nu_{\text{th}i})/c\sim\nu_{\text{the}}/c]\ll 1$, and the $\epsilon\{=1-[(\omega_{pe}^2+\omega_{pi}^2)/\omega^2]\sim 1-(\omega_{pe}^2/\omega^2)\}$ is the dielectric constant.

(c) The laser wavelength (λ_{ls}) is greater than the electrostatic wavelength (λ_{es}), and also the thermal velocities (v_{the} and $v_{\text{th}i}$) and the Debye length (λ_D) are small compared with the phase velocity (v_{φ}) of the radiation field and the density scale length (L) of the plasma, respectively. The effect of plasma inhomogeneity may therefore be neglected.

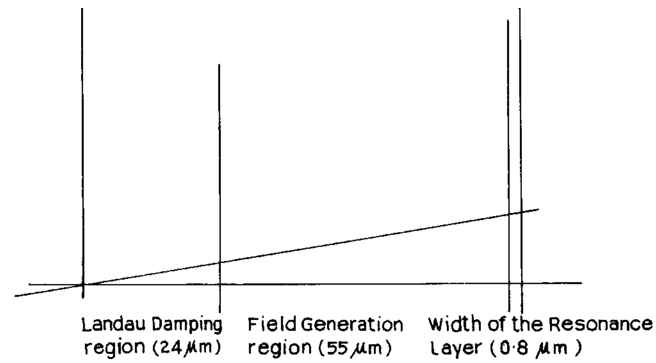

FIG. 5. A rough sketch for different regions out of the characteristic length (L) 80 μm.

Hence, assuming a typical value of the plasma temperature of 3 keV, the dimensionless amplitude of the electrostatic mode $\alpha_{\parallel}$ can be estimated quantitatively typically of the order of 10^{-3}. This leads us to conclude that about 3.8% of the laser light would be converted to the electrostatic mode in an underdense plasma having 3-keV temperature (say). This is the main source of poloidal fields [30,31].

Our results have the consequences of the inverse Faraday effect (IFB) [40] because in an IFE process the kinetic energy of the ordered motion of particles in the presence of an electromagnetic wave is transformed into the energy of the induced magnetic field. The field generation mechanism in our study is a direct process due to the fact that, to calculate induced magnetic fields, we have calculated the average nonlinear angular momentum of electrons and ions via the nonlinear electron and ion velocities and their displacements, whereas the IFE is an indirect process of the field generation.

Our mechanism is different from the dynamo effect [15,16] because our results, showing the simultaneous generation of toroidal and poloidal magnetic fields, do not produce cyclically as toroidal to poloidal fields and vice versa.

The temperature distribution of charge particles in plasmas is assumed to be uniform (i.e., $T_e=T_i=T$) and so the temperature gradient is absent (i.e., $\nabla T=0$), hence the thermoelectric effects [1,23] are automatically suppressed in our model.

The electrostatic mode (i.e., the wake field) generation in an underdense plasma is also of current interest, with the advent of ultrashort pulse lasers, because such fields play an important role in plasma-based accelerators [41]. Such wake fields are also important for the production of magnetic fields in laser-produced plasmas [41,42]. All these will be studied elsewhere.

Uniform compression of a spherical target is one of the key issues for inertial confinement fusion. The coupling of the self-induced magnetic fields with the transport processes may have serious effects on the heat flux, but this has not been investigated in detail because of its complexity. When the toroidal fields of the megagauss range were observed in laser plasmas, it was realized that such toroidal fields enhance the lateral energy transport [24–29] but the axial energy propagation due to the poloidal field was ignored. In fact, the rate of energy deposition and inhibition in the conduction region due to poloidal fields is yet to be studied thoroughly. Moreover, electrons and ions turn around the toroidal and poloidal fields and get trapped in a layer of the radius of the order of their Larmor radii. Ion's Larmor radius is greater than that of the electron in the presence of a magnetic field. The strong toroidal field (of the order of several megagauss) enhances lateral energy transport but degrades axial energy transport which affects the implosion physics of the ICF target [24–26]. But the poloidal field, though weak, can trap both electrons and ions along the axis of the laser beam. Ideally it is desirable that the rate of energy deposition, due to poloidal fields in conduction regions, should be increased, thereby enhancing the energy transport from the critical surface to the ablation surface. Hence, the energy distribution in conduction regions due to toroidal and poloidal fields are important. It may be speculated that the poloidal field combined with the toroidal field set up by the laser may lead to the formation of a magnetic cage which could be used for plasma confinement such as a spheromak and also for better thermal insulation in an inertial confinement scheme [43].

ACKNOWLEDGMENTS

The authors would like to thank Professor P. Kull, Technische Hochschule Aachen, Germany, for his valuable suggestions and stimulating discussions. One of the authors (B.B.) would also like to thank Professor P. Mulser, Technische Hochschule Darmstadt, Germany, for useful suggestions and also for providing local hospitality during his stay at Darmstadt. This work was supported by the Department of Science and Technology, India.

APPENDIX A: FIRST-ORDER HARMONIC TERMS CORRECT UP TO THIRD ORDER

Integrating Eqs. (29) and (30) the expressions for the displacements of the electron and ion can be written, by retaining only first-order harmonic terms correct up to third order [37,38], as in the following:

$$\begin{aligned} r_{e3}=i\left(\frac{c}{2\omega}\right)&\{\hat{\mathbf{x}}[R_{11}\alpha_\parallel^3 e^{i\theta_\parallel}+R_{12}(\alpha_\perp^2-\beta_\perp^2)\alpha_\parallel e^{i(2\theta_\perp-\theta_\parallel)}\\ &+R_{13}(\alpha_\perp^2+\beta_\perp^2)\alpha_\parallel e^{i\theta_\parallel}]+\hat{\mathbf{y}}[R_{21}\alpha_\parallel^2\alpha_\perp e^{i(2\theta_\parallel-\theta_\perp)}\\ &+R_{22}(\alpha_\perp^2-\beta_\perp^2)\alpha_\perp e^{i\theta_\perp}+R_{23}\alpha_\parallel^2\alpha_\perp e^{i\theta_\perp}]\\ &-i\hat{\mathbf{z}}[R_{31}\alpha_\parallel^2\beta_\perp e^{i(2\theta_\parallel-\theta_\perp)}+R_{32}(\alpha_\perp^2-\beta_\perp^2)\beta_\perp e^{i(2\theta_\perp-\theta_\perp)}\\ &+R_{33}\alpha_\parallel^2\beta_\perp e^{i\theta_\perp}]\}+\text{c.c.} \end{aligned} \quad \text{(A1)}$$

and

$$\begin{aligned} r_{i3}=i\left(\frac{c}{2\omega}\right)&\{\hat{\mathbf{x}}[T_{11}\alpha_\parallel^3 e^{i\theta_\parallel}+T_{12}(\alpha_\perp^2-\beta_\perp^2)\alpha_\parallel e^{i(2\theta_\perp-\theta_\parallel)}\\ &+T_{13}(\alpha_\perp^2+\beta_\perp^2)\alpha_\parallel e^{i\theta_\parallel}]+\hat{\mathbf{y}}[T_{21}\alpha_\parallel^2\alpha_\perp e^{i(2\theta_\parallel-\theta_\perp)}\\ &+T_{22}(\alpha_\perp^2-\beta_\perp^2)\alpha_\perp e^{i\theta_\perp}+T_{23}\alpha_\parallel^2\alpha_\perp e^{i\theta_\perp}]\\ &-i\hat{\mathbf{z}}[T_{31}\alpha_\parallel^2\beta_\perp e^{i(2\theta_\parallel-\theta_\perp)}+T_{32}(\alpha_\perp^2-\beta_\perp^2)\beta_\perp e^{i\theta_\perp}\\ &+T_{33}\alpha_\parallel^2\beta_\perp e^{i\theta_\perp}]\}+\text{c.c.}, \end{aligned} \quad \text{(A2)}$$

where $R_{11}=P_{11}/Q_{11}$, $R_{12}=P_{12}/Q_{12}$, $R_{13}=P_{13}/Q_{13}$,

$$\begin{aligned} P_{11}=\{&A_{e1}[n_\parallel^2(V_i^2/2)-1+X_i]+X_eA_{i1}\\ &-M_e(\sigma_{11}+\Gamma_{11})[n_\parallel^2(V_i^2/2)-1]\}, \end{aligned}$$

$$\begin{aligned} P_{12}=\{&A_{e2}[(2n_\perp-n_\parallel)^2(V_i^2/2)-1+X_i]+X_eA_{i2}\\ &-M_e(\sigma_{21}+\Gamma_{21})[(2n_\perp-n_\parallel)^2(V_1^2/2)-1]\}, \end{aligned}$$

$$P_{13}=\{A_{e3}[n_\perp^2(V_1^2/2)-1+X_i]+X_eA_{i3}\},$$

$$\begin{aligned} Q_{11}=\{&[n_\parallel^2(V_i^2/2)-1][n_\parallel^2(v_e^2/2)-1]+X_e[n_\parallel^2(V_i^2/2)-1]\\ &+X_i[n_\parallel^2(V_e^2/2)-1]\}, \end{aligned}$$

$$\begin{aligned} Q_{12}=\{&[n_\parallel^2(V_i^2/2)-1][n_\parallel^2(V_e^2/2)-1]+X_e[n_\parallel^2(V_i^2/2)-1]\\ &+X_i[n_\parallel^2(V_e^2/2)-1]\}, \end{aligned}$$

$$\begin{aligned} Q_{13}=\{&[n_\parallel^2(V_i^2/2)-1]+[n_\parallel^2(V_e^2/2)-1]+X_e[n_\parallel^2(V_i^2/2)-1]\\ &+X_i[n_\parallel^2(V_e^2/2)-1]\} \end{aligned}$$

and

$$R_{21}=P_{21}/Q_{21},\quad R_{22}=P_{22}/Q_{22},\quad R_{23}=P_{23}/Q_{23},$$

$$P_{21}=[M_e\sigma_{31}],\quad P_{22}=[M_e\sigma_{41}],$$

$$P_{23}=\{\rho_{e4}[n_1^2-1+X_i]+X_e\rho_{i4}-M_e\Gamma_{31}\},$$

$$Q_{21}=[n_1^2-1+X_i+X_e],\quad Q_{22}=[n_\perp^2-1+X_i+X_e],$$

$$Q_{23}=[n_\perp^2-1+X_i+X_e],$$

$$R_{31}=P_{31}/Q_{31},\quad R_{32}=P_{32}/Q_{32},\quad R_{33}=P_{33}/Q_{33},$$

$$P_{31}=P_{21},\quad P_{32}=P_{22},\quad P_{33}=-P_{23}$$

$$Q_{31}=Q_{21},\quad Q_{32}=Q_{22},\quad Q_{33}=Q_{23}.$$

Also we have

$$T_{11}=S_{11}/L_{11},\quad T_{12}=S_{12}/L_{12},\quad T_{13}=S_{13}/L_{13},$$

$$\begin{aligned} S_{11}=\{&A_{il}[n_\parallel^2(V_e^2/2)-1+X_e]+X_iA_{e1}\\ &+M_i(\sigma_{11}+\Gamma_{11})[n_\parallel^2(V_e^2/2)-1]\}, \end{aligned}$$

$$S_{12}=\{A_{i2}[(2n_{\perp}-n_{\parallel})^2(V_e^2/2)-1+X]+X_iA_{e2}+M_i(\sigma_{21}+\Gamma_{21})[(2n_{\perp}-n_{\parallel})^2(V_e^2/2)-1]\},$$

$$S_{13}=\{A_{i3}[n_{\parallel}^2(V_e^2/2)-1+X]+X_iA_{e3}\},$$

$$L_{11}=\{[n_{\parallel}^2(V_i^2/2)-1][n_{\parallel}^2(V_e^2/2)-1]+X_e[n_{\parallel}^2(V_i^2/2)-1]+X_i[n_{\parallel}^2(V_e^2/2)-1]\},$$

$$L_{12}=\{[(2n_{\perp}-n_{\parallel})^2(V_i^2/2)-1][(2n_{\perp}-n_{\parallel})^2(V_e^2/2)-1]+X_e[(2n_{\perp}-n_{\parallel})^2(V_i^2/2)-1]+X_i[(2n_{\perp}-n_{\parallel})^2(V_e^2/2)-1]\},$$

$$L_{13}=L_{11},$$

$$T_{21}=S_{21}/L_{21},\quad T_{22}=S_{22}/L_{22},\quad T_{23}=S_{23}/L_{23},$$

$$S_{21}=[M_i\sigma_{31}],\quad S_{22}=[M_i\sigma_{41}],$$

$$S_{23}=[\rho_{i4}(n_{\parallel}^2-1+X_e)+X_i\rho_{e4}-M_i\Gamma_{31}],$$

$$L_{21}=[n_{\parallel}^2-1+X_i+X_e],\quad L_{22}=[n_{\perp}^2-1+X_i+X_e],$$

$$L_{23}=[n_{\perp}^2-1+X_i+X_e],$$

$$T_{31}=S_{31}/L_{31},\quad T_{32}=S_{32}/L_{32},\quad T_{33}=S_{33}/L_{33},$$

$$S_{31}=S_{21},\quad S_{32}=S_{22},\quad S_{33}=-S_{23},$$

$$L_{31}=L_{21},\quad L_{32}=L_{22},\quad L_{33}=L_{23},$$

APPENDIX B: ELECTROSTATIC WAVE AND LANDAU DAMPING (Ref. [31])

It is a fact that the fluid description neglects Landau damping of an electrostatic wave in laser plasmas, but in the Vlasov-Maxwell theory, it can be shown easily from the dispersion relation that the Landau damping exists outside the resonance layer (Δx) and that the distance over which the electrostatic wave freely propagates can be estimated in a reasonable order of magnitude. By taking the dispersion relation [44] in the following form:

$$D(\omega,k)=1-\Sigma\left(\frac{\omega_{pe,i}^2}{k^2}\right)\int\frac{(\partial F_{e,i}/\partial u)}{u-\omega/k}du=0, \tag{B1}$$

all symbols have their usual meanings. Generally, Eq. (B1) relates complex number such that

$$D(\omega,k)=D_r(\omega,k)+iD_i(\omega,k), \tag{B2}$$

where the subscripts r and i represent the real and imaginary part of the dispersion relation (B1), respectively. Let the complex wave number and complex frequency be

$$k=k_r+ik_i \quad \text{and} \quad \omega=\omega_r+\omega_i. \tag{B3}$$

Assuming the imaginary parts are small, i.e.,

$$\omega_i/\omega_r\ll 1 \quad \text{and} \quad k_i/k_r\ll 1. \tag{B4}$$

Expanding Eq. (B2) about real frequency and real wave number, and separating the real part and imaginary parts we get

$$D_r(\omega_r,k_r)=0, \tag{B5}$$

$$\partial_{\omega_i}D_r(\omega_r,k_r)\omega_i+\partial_{k_r}D_r(\omega_r,k_r)k_i+D_i(\omega_r,k_r)=0, \tag{B6}$$

where

$$D_r(\omega,k)\equiv 1-\Sigma\left(\frac{\omega_{pe,i}^2}{k^2}\right)\int_c\frac{(\partial F_{e,i}/\partial u)}{u-\omega_r/k_r}du, \tag{B7}$$

$$D_i(\omega,k)=-\pi\Sigma\left(\frac{\omega_{pe,i}^2}{k^2}\right)\left(\frac{\partial F_{e,i}(\omega_r/k_r)}{\partial u}\right), \tag{B8}$$

where c is the Landau contour.[1]

For the mode conversion analysis we take the frequency as

$$\omega_r=\omega,\quad \omega_i=0, \tag{B9}$$

and also assuming the distribution function is Maxwellian then we have

$$f_{e,i}=\Sigma\left(\frac{m_{e,i}}{2\pi KT_{e,i}}\right)^{3/2}\exp\left(-\frac{m_{e,i}u^2}{2KT_{e,i}}\right). \tag{B10}$$

By neglecting ion terms, which are small by m_e/m_i, the integral of Eq. (B7) may be evaluated explicitly for fluid approximations as

$$D_r=\epsilon-\frac{v_{\text{the}}^2k_r^2}{\omega^2}, \tag{B11}$$

$$D_i=3^{3/2}(\pi/2)^{1/2}\epsilon^{-3/2}\exp\left(-\frac{3}{2}\frac{1}{\epsilon}\right), \tag{B12}$$

where Eq. (B11) is the real dispersion relation which follows directly from Eq. (19) if the ion distribution is dropped, and Eq. (B12) gives the dispersion relation for an imaginary effect.

One then readily obtains the expression for the real wave number as

$$k_r=\frac{k_0\sqrt{\epsilon}}{V_e} \tag{B13}$$

and for the imaginary wave number as

[1]Equation (B1) is similar to equation 8.3.11 [44], if the electrostatic case only be retained, and the function $F_{e,i}$ is the integral of the distribution function of f_{ei} defined in Ref. [44]. Moreover, Eqs. 8.6.11 and 8.6.12 [44] may be expressed as Eqs. (B7) and (B8), respectively, for real (ω_r) and real (k_r).

$$k_i=\frac{-1}{V_e\sqrt{\epsilon}}\,\omega_{pe}\sqrt{\frac{\pi}{8}}\left[\left(\frac{3}{\epsilon}\right)\exp\left(-\frac{1}{\epsilon}\right)\right]^{3/2}, \tag{B14}$$

where k_0 is the vacuum wavelength and $\epsilon=1-(\omega_{pe}^2/\omega^2)$.

Therefore, the wave amplitude then decreases by the factor $\exp(-\psi)$ where the damping argument ψ is of the form

$$\Psi=\int k_i dz. \tag{B15}$$

For a linear profile $\epsilon=z/L$, we have the damping argument as

$$\psi=\sqrt{\frac{3}{2}\pi}\left(\frac{k_0L}{V_e}\right)\exp\left[-\frac{3}{2}\frac{1}{\epsilon}\right], \tag{B16}$$

which is to be a linear function of (k_0L/V_e) only when the density is fixed.

Moreover, for the same profile we have the following:

$$\int k_r dz=\left(\tfrac{2}{3}\right)\xi^{3/2}. \tag{B17}$$

Let n be the number of the electrostatic wavelength, which can be expressed easily as

$$n=(1/3\pi)\xi^{3/2}. \tag{B18}$$

The above equation (B18) allows us to choose the number of electrostatic wavelength as $n\simeq 24$ and consequently, we have from Eq. (B17) that the effective region of Landau damping is approximately 24 μm for the linear profile $\epsilon \simeq 0.25$. Moreover, we also have the thickness of the resonance layer $\Delta x\simeq 0.8\,\mu$m. So, the magnetic fields are calculated only on the region of typical length 55 μm. In other words, magnetic fields at the resonance layer and also at the Landau damping region have not been included in our present analysis. This should be done elsewhere. A rough sketch has been given in Fig. 5 for understanding the region of our interest in magnetic-field calculations.

[1] J. A. Stamper, K. Papadopoulus, R. N. Sudan, S. O. Dean, E. A. McLean, and J. M. Dawson, Phys. Rev. Lett. **26**, 1012 (1972).
[2] P. Mora and R. Pellat, Phys. Fluids **24**, 2219 (1981); **24**, 2227 (1981).
[3] W. Woo and J. S. DeGroot, Phys. Fluids **21**, 124 (1978); **21**, 2072 (1978).
[4] T. Yabe, Y. Kitagawa, A. Ishizaki, M. Naito, A. Nishiguchi, M. Yokoyama, and C. Yamanaka, Phys. Rev. Lett. **51**, 1869 (1983).
[5] A. Raven, P. T. Rumsby, J. A. Stamper, O. Willi, R. Illingworth, and R. Tharaja, Appl. Phys. Lett. **35**, 526 (1979).
[6] N. K. Winsor and D. A. Tidman, Phys. Rev. Lett. **31**, 1044 (1973).
[7] T. Yabe, K. Mima, T. Sugiyama, and K. Yoshikawa, Phys. Rev. Lett. **48**, 242 (1982).
[8] B. Greek, P. Martin, T. W. Johnston, H. Pepin, G. Mitchell, and F. Reheat, Phys. Rev. Lett. **41**, 1811 (1978).
[9] I. Speziale and P. J. Catto, Phys. Fluids **21**, 2063 (1978).
[10] J. A. Stamper and D. A. Tidman, Phys. Fluids **16**, 2024 (1973).
[11] B. Bezzerides, D. F. DuBois, D. W. Forslund, and E. L. Lindman, Phys. Rev. Lett. **38**, 495 (1977).
[12] K. Estabrook, Phys. Rev. Lett. **41**, 1808 (1978).
[13] A. Ramani and G. Laval, Phys. Fluids **21**, 980 (1978).
[14] J. Briand, V. Adrian, M. El. Tamer, A. Gomes, Y. Quemener, J. P. Dinguirard, and J. C. Kieffer, Phys. Rev. Lett. **54**, 38 (1985).
[15] R. Dragila, Phys. Fluids **30**, 925 (1978).
[16] V. Y. Bychenkov, O. M. Gradov, and G. A. Chokparova, Fiz. Plazmy **10**, 741 (1984) [Sov. J. Plasma Phys. **10**, 430 (1984)].
[17] B. Chakraborty, M. Khan, B. Bhattacharyya, S. Dev, and H. C. Pant, Phys. Fluids **31**, 1303 (1988).
[18] B. Bera, C. Das, B. Chakraborty, V. Krishan, and B. Bhattacharyya, Int. J. Theor. Phys. **31**, 1295 (1992).
[19] B. Bhattacharyya, Phys. Lett. A **185**, 333 (1994).
[20] C. Das, B. Bera, B. Chakraborty, and M. Khan, J. Plasma Phys. **50**, 191 (1994).
[21] M. Khan, C. Das, B. Chakraborty, T. Desai, H. C. Pant, M. K. Srivastava, and S. V. Lawande, Phys. Rev. E **58**, 925 (1998).
[22] R. N. Sudan, Phys. Rev. Lett. **70**, 3075 (1993).
[23] J. A. Stamper, Laser Part. Beams **9**, 841 (1991).
[24] W. C. Mead, E. M. Campbell, W. L. Kruer, R. E. Turner, C. W. Hatcher, D. S. Baileg, P. H. Y. Lee, J. Foster, K. G. Tirsell, B. Pruett, N. C. Holmes, J. T. Trainor, G. L. Stradling, B. F. Lasinski, C. E. Max, and F. Ze, Phys. Fluids **27**, 1301 (1984).
[25] C. E. Max, W. M. Manheimer, and J. J. Thomson, Phys. Fluids **21**, 128 (1978).
[26] C. E. Max, in *Laser Plasma Interaction*, edited by R. Ballan and J. C. Admes (North-Holland, Amsterdam, 1982), Vol. 34, pp. 356–386.
[27] I. P. Shkarofsky, Phys. Fluids **23**, 52 (1980).
[28] I. B. Bernstein, C. M. Max, and J. J. Thomson, Phys. Fluids **21**, 905 (1978).
[29] J. H. Nuckolls, in *Laser Interaction and Releated Phenomena* (Plenum, New York, 1974), Vol. **3B**, pp. 399.
[30] B. Bhattacharyya and Urmi Sanyal, J. Plasma Phys. **60**, 21 (1999).
[31] H. J. Kull, Ph.D. thesis, Max-Planck-Institut fur Quantenoptik, Garching, Germany, 1981; Phys. Fluids **26**, 1881 (1983).
[32] W. L. Kruer, *The Physics of Laser Plasma Interactions* (Addison-Wesley, New York, 1987).
[33] Y. R. Shen, Mod. Phys. **48**, 1 (1976).
[34] A. C. Newell and J. V. Moloney (Addison-Wesley, New York, 1992), Chap. 2.
[35] Yu. M. Aliev, Yu. V. Bychenkov, and S. Vukovic, J. Plasma Phys. **48**, 325 (1992).
[36] R. P. Bellman, *Perturbation Technique in Mathematics, Physics and Engineering* (Holt, Rinehart and Winston, New York, 1964), pp. 57.
[37] B. Chakraborty, S. N. Paul, M. Khan, and B. Bhattacharyya, Phys. Rep. **114**, 181 (1984).

[38] R. Y. Chiao and J. Godine, Phys. Rev. **185**, 430 (1969).
[39] T. J. M. Boyd, G. J. Humphreys-Jones, and D. Corks, Phys. Lett. **88A**, 140 (1982).
[40] A. D. Steiger and C. H. Wood, Phys. Rev. A **5**, 467 (1972).
[41] E. Esare, P. Sprangle, J. Krall, and A. Ting, IEEE Trans. Plasma Sci. **24**, 252 (1996).
[42] L. Gorbunov, P. Mora, and T. M. Antonsen, Jr., Phys. Rev. Lett. **76**, 2495 (1996); Phys. Plasmas **4**, 4358 (1997).
[43] A. Hasegawa, K. Nishihara, H. Daido, M. Fujita, A. Ishizaki, F. Miki, K. Mima, M. Murakami, S. Nakai, K. Terai, and C. Yamanaka, Nucl. Fusion **28**, 369 (1988).
[44] N. A. Krall and T. W. Trivelpiece, *Principles of Plasma Physics* (McGraw-Hill, New York, 1973).